Metastability of Corundum-Type In_2O_3

Aleksander Gurlo,*[a] Peter Kroll,[b] and Ralf Riedel[a]

Abstract: The description of structural relations between bixbyite- and corundum-type structures is of particular interest because of the common occurrence of both structures. One of the representative examples of the bixbyite to corundum transition is the high-pressure high-temperature synthesis of the corundum-type indium oxide. The wet chemistry synthesis and stabilisation of the corundum-type In_2O_3 under ambient pressure conditions calls for a re-interpretation of the In−O phase diagram as well as for the clarification of the phase transitions in In_2O_3. One of the questions to be clarified is the stability of the corundum-type In_2O_3. In the present work we studied the stability of the corundum-type In_2O_3 both theoretically (by density-functional calculations) and experimentally. The synthesis of the corundum-type In_2O_3 was performed by the modified non-alkoxide sol–gel method based on the ammonia-induced hydrolysis of indium nitrate in methanol. The corundum-type In_2O_3 was subjected to thermal analysis (STA) as well as to structural studies, that is, it was examined using X-ray powder diffraction (XRPD) including in situ XRPD characterisation upon thermal treatment. For the first time we have undoubtedly demonstrated,

Keywords: ab initio calculations · indium oxide · indium · metastable compounds · phase transitions

both theoretically and experimentally, the metastability of the corundum-type In_2O_3 polymorph. The In_2O_3 polymorph appears to be metastable throughout the entire enthalpy–pressure phase diagram. Upon heating, corundum-type In_2O_3 transforms irreversibly into cubic bixbyite-type In_2O_3 as shown by STA as well as in situ heating XRPD experiments. Computations indicate the existence of another high-pressure modification of In_2O_3 with orthorhombic structure, iso-typic to Rh_2O_3-II. We predict this new phase to form at pressures exceeding 15 GPa from both the cubic bixbyite-type and the corundum-type modification of In_2O_3.

Introduction

The bixbyite- (space group $Ia\bar{3}$, No. 204) and corundum-type (space group $R\bar{3}c$, No. 167) structures are important for their common occurrence, that is, the majority of trivalent rare-earth oxides crystallise in the bixbyite-type and the majority of the transition metal oxides assume the corundum-type structure. Some of the sesquioxides, such as Fe_2O_3, Cr_2O_3 and Tl_2O_3, can adopt both structures. The bixbyite- and corundum-type structures are also illustrative textbook examples for teaching crystal-building principles. The structural relations as well as the possible transformation mechanisms from bixbyite to corundum have attracted significant attention over the years. The latter can be treated as a particular case of the distorted ccp→hcp transition (ccp and hcp: cubic and hexagonal close-packed structures, respectively), which is described in terms either of continuous topological variation of atom coordination[1,2] or continuous displacement of the atoms.[3]

One of the representative examples of the bixbyite to corundum transition is the high-pressure high-temperature synthesis of the corundum-type indium oxide (In_2O_3).[4–7] Under normal conditions In_2O_3 crystallises in the cubic bixbyite-type structure (denoted as c-In_2O_3 hereafter). Corundum-type indium(III) oxide (denoted as rh-In_2O_3 hereafter) is known to be a high-pressure In_2O_3 polymorph. The fundamental understanding of the phase transitions in the In−O-system as well as of the stability of different polymorphic modifications of indium oxide has a particular significance. This is caused by the technological importance of In_2O_3 in many application fields, for example, in photovoltaics (transparent conducting electrodes[8]), gas detection (con-

[a] Dr. A. Gurlo, Prof. Dr. R. Riedel
Fachbereich Material- und Geowissenschaften
Technische Universitaet Darmstadt
Petersenstr. 23, 64287 Darmstadt (Germany)
Fax: (+49)6151-166346
E-mail: gurlo@materials.tu-darmstadt.de

[b] Prof. Dr. P. Kroll
Department of Chemistry and Biochemistry
The University of Texas at Arlington
Arlington, Texas 760019–0065 (USA)

ductometric gas sensors[9]), nanoelectronics (field effect transistors based on quasi one dimensional structures[10]). Moreover, the knowledge about the phase transitions in In_2O_3 has remarkable relevance to the understanding of phase equilibria in the In_2O_3–SnO_2 (ITO) system.[11] However, there is notable less data available concerning 1) the experimental aspects of the bixbyite to corundum transition[6,12] and 2) the stability of the In_2O_3 polymorphs.[13]

To the best of our knowledge, the first synthesis of the rh-In_2O_3 was reported by Shannon in 1966;[4] he applied high-pressure/high-temperature conditions (6.5 GPa, 1250 °C) to obtain corundum-type In_2O_3. In 1969 Rind and Ringwood reported the stability of rh-In_2O_3 up to 12 GPa and 900 °C.[5] In the same year Shannon et al. observed formation of rh-In_2O_3 in quenched (after 6.5 GPa and 800–1250 °C) solid solutions of In_2O_3–Tl_2O_3, In_2O_3–Sc_2O_3, and In_2O_3–Fe_2O_3.[6] In 1990 Atou et al. reported the shock induced phase transition to rh-In_2O_3 at 15–25 GPa.[7] In all works on high-pressure synthesis of rh-In_2O_3[4–7] the conclusions about the phase transitions in In_2O_3 as well as about the stability of the rh-In_2O_3 under high-pressure conditions were drawn from the identification of the quenched products. Herein it was assumed that "the presence of large crystals suggests that rapid reconstructive transformation did not take place".[6]

Even if the rh-In_2O_3 is traditionally thought to be a high-pressure In_2O_3 polymorph, recent works show that rh-In_2O_3 can also crystallise at ambient pressure conditions ("ambient" rh-In_2O_3 hereafter) (see also Table 1). The number of works reporting the synthesis of the "ambient" rh-In_2O_3 has been continuously increasing during last years. Thus, rh-In_2O_3 was found 1) in quasi one-dimensional nanostructures (nanorods,[14,15] nanowires,[16] nanofibers,[17] nanotubes[18]), 2) as a product of the calcination of the InOOH at elevated temperatures (300–600 °C)[14,15,17–22] and 3) in the sol–gel synthesised In_2O_3.[23–25] The stabilisation of the rh-In_2O_3 structure under ambient pressure was also observed 1) in the solid solutions In_2O_3–SnO_2[22,26–31] and In_2O_3-Fe_2O_3,[32–34] 2) in epitaxial films grown in MOCVD on sapphire (corundum-type Al_2O_3) substrates[35] and in nitrogen-doped In_2O_3 thin films.[36]

The low-temperature/ambient-pressure synthesis and stabilisation of the rh-In_2O_3 calls for a re-interpretation of the In−O phase diagram as well as for the clarification of the phase transitions in In_2O_3. The main problem is the lack of the reliable experimental data. Hitherto there are only three independent reports on the high-pressure/high-temperature behaviour of In−O phases (see above), two of them date from the 1960s. The information about the thermal stability of the rh-In_2O_3 is controversial. Corundum-type In_2O_3 was assumed to be metastable (1967,[37]). This assumption, however, was never proven experimentally on rh-In_2O_3. For solid-solutions it was found that the In_2O_3–SnO_2 with corundum structure decomposes at temperatures > 900 °C to c-In_2O_3 and SnO_2.[26] On other evidence, they transform at 800 °C into bixbyite-type structure.[27] Even if several recent works are entitled "metastable hexagonal In_2O_3",[17,20] they do not address the stability aspects of rh-In_2O_3. Moreover, in the synthesis of the "ambient" rh-In_2O_3 the final thermal treatment was limited to short times (1–2 h) and low temperatures, for example, 1) 600 °C as maximum calcination temperature;[14] 2) 500 °C as a maximum temperature in the thermal analysis.[19] Even if the thermal analysis was performed up to 900 °C[17] (only one work reporting such high-temperature treatment), the phase composition of the products was not determined. The appearance of the rh-In_2O_3 after low-temperature treatment of the sol–gel synthesised In_2O_3,[24,25] hitherto, remained unexplained.

Thus, the rh-In_2O_3 obtained according to the method described in the ref. [23] and calcined at 500 °C for 1 h in air was used in the present work for the structural studies, that is, was examined by using X-ray powder diffraction (XRPD) including also in situ characterisation upon thermal treatment.

Results and Discussion

Structure refinement of the corundum-type In_2O_3: XRPD examination of the as-prepared sample shows diffraction patterns that can undoubtedly be attributed to that of rh-In_2O_3 (Figure 1A, Table 2). A full-profile Rietveld structure refinement (using the program FullProf) verified the lattice parameters of the rh-In_2O_3. On heating up to 700 °C in air for 1 h and cooling to room temperature, the corundum-type rh-In_2O_3 transforms irreversibly to cubic c-In_2O_3 (Figure 1B).

Table 1. Synthesis of the corundum-type In_2O_3.

| Synthesis	Precursors/reactions	Conditions/Systems	Refs
high-pressure high-temperature	c-In_2O_3	65 kbar (6.5 GPa), 800–1250 °C	[4,6]
		shock induced; 15–25 GPa	[7]
		120 kbar (12 GPa), 900 °C	[5]
hydrothermal	Na_2O-$In(OH)_3$ (or c-In_2O_3)-H_2O (NaOH flux)	300–1000 bar[a]; 350–400 °C	[37,38]
	In_2O_3 + NaOH flux	44 kbar; 350–400 °C	[6]
calcination	InOOH	300–600 °C	[14,15,17–22]
precipitation	In^{3+} (indium nitrate) methanol/water, $NH_3 \times H_2O$	1 bar, 250 °C[b]	[23–25]
epitaxial growth	trimethylindium; MOCVD	[0001]In_2O_3 [0001]Al_2O_3	[35]
stabilisation in solid solutions	in most cases: coprecipitation	In_2O_3–SnO_2	[22,26–31]
		In_2O_3–Fe_2O_3	[32–34]

[a] Coexistence with InOOH. [b] Traces.
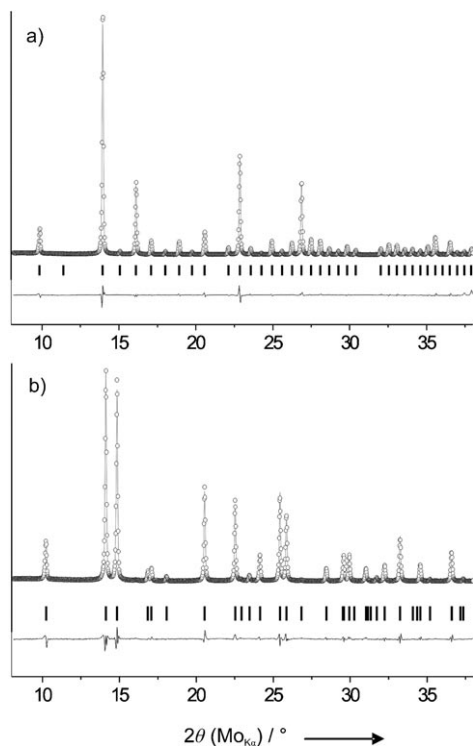
Figure 1. XRPD pattern for a) rh-In_2O_3 and b) c-In_2O_3 (after heating of the rh-In_2O_3 at 700 °C for 1 h) observed (open circles) and calculated (solid line, Rietveld refinement) intensities. Their difference curve is given at the bottom of the graph. The calculated peak positions are denoted by tick marks.

Table 2. Structural parameters of rh- and c-In_2O_3 (Rietveld refinement results, see Figure 1 A,B).

Parameter	rh-In_2O_3	c-In_2O_3
structure type	corundum	bixbyite
space group (No Int Tables)	$R\bar{3}c$ (167)	$Ia\bar{3}$ (204)
lattice parameters [Å]		
a	5.491(1)	10.126(7)
b	5.491(1)	–
c	14.526(1)	–
V [Å³]/In_2O_3	63.22(5)	64.89(1)

Thermal analysis and in-situ XRPD: The simultaneous thermogravimetry/differential scanning calorimetry (STA) investigation shows that between 500 and 650 °C rh-In_2O_3 transforms irreversibly into c-In_2O_3 (phase composition of final material was verified by XRPD). Herein no sharp peaks were observed indicating very small difference in the heat capacity of the two indium oxide polymorphs. According to the STA results it is not possible to assign any critical transformation temperature to the irreversible transformation rh-$In_2O_3 \rightarrow$ c-In_2O_3. The results of the STA investigation with simultaneous gas analysis, that is, no change in the mass of the sample as well as no gas evolution during the heating and cooling, shows that the "ambient" rh-In_2O_3 does not include any additional inorganic or organic additives (molecules, radicals) for stabilizing the corundum-type structure of the "ambient" rh-In_2O_3 (Figure 2).
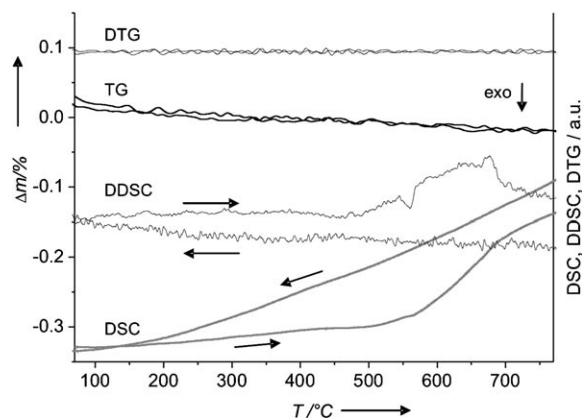

Figure 2. STA results indicating an irreversible phase transition in the heating run between 500 and 650 °C. Simultaneous gas analysis does not show any gas evolution in the heating and cooling runs.

According to the thermophysical data (for both phases: Madelung constants and electrostatic energy;[6] for c-In_2O_3: the heat capacity dependence on the temperature[39] and standard enthalpy of formation -923.5 kJ mol^{-1}[40]), one would expect an exothermic effect if rh-In_2O_3 transforms into c-In_2O_3 (Δ_{trs}, H is of about -25 kJ mol^{-1}). Because the thermal evolution of metastable phases clearly depends on temperature, and/or on the rate at which the temperature is increased, or both,[41] the rh-$In_2O_3 \rightarrow$ c-In_2O_3 transition will be a function of both temperature and time. By monitoring the decrease in the intensity of the (104) and (110) reflections of rh-In_2O_3 and increase in the intensity of the (222) reflection of the c-In_2O_3 in the in situ heating XRPD experiments, one can see how the rh-In_2O_3 transforms irreversibly into c-In_2O_3 (Figure 3). Herein the time of the full transition is around 2 h.

Density-functional calculations—prediction of a new In_2O_3 polymorph: The density-functional calculations show that the cubic bixbyite-type structure is indeed the ground state
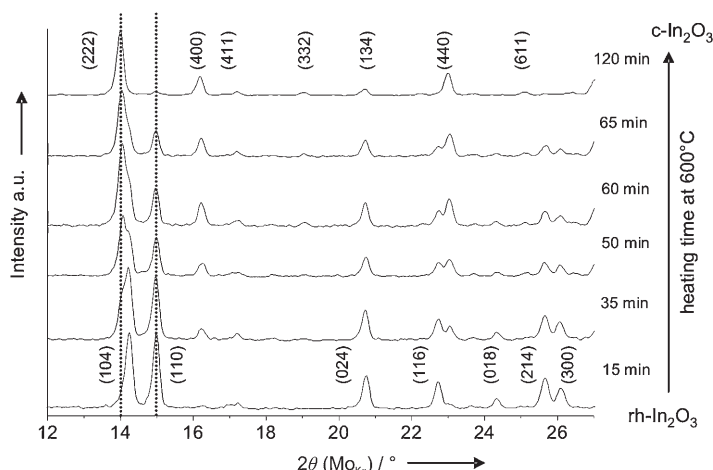

Figure 3. In situ XRPD patterns (only a selected part is shown) of the rh-In_2O_3 upon heating at 600 °C in air. The diffraction pattern of the sample heated for 120 min does not change after cooling to room temperature.

structure of In_2O_3 and that the hexagonal corundum-type modification is metastable at ambient pressure (Figure 4).
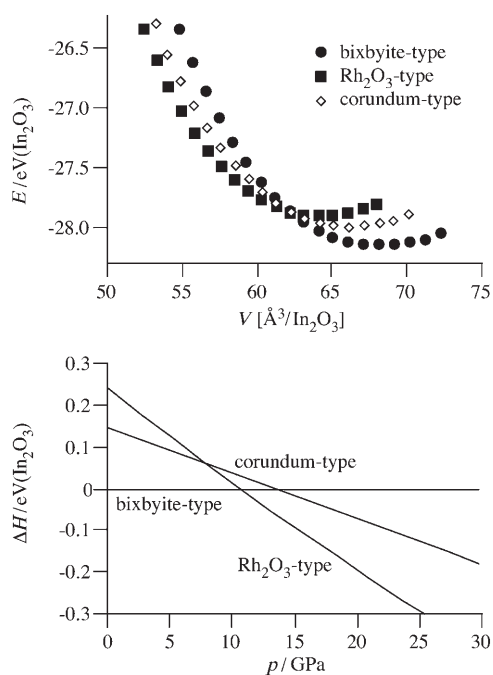

Figure 4. The energy–volume diagram (top) and the enthalpy–pressure diagram (bottom) for indium oxide polymorphs. c-In_2O_3 (bixbyite) is a reference structure in the lower diagram.

The enthalpy difference of 15 kJ mol^{-1} that we compute at ambient pressure relates well to the experimental calorimetric data observed in the STA. Upon compression the enthalpy difference between these two phases decreases, and eventually at 13.5 GPa the enthalpy of both phases become equal, indicating a phase transition. We note that our value for the transition pressure is higher than the 3.8 GPa derived in recent calculations.[13] However, while these have been carried out using the local density approximation (LDA), common experience favours the generalised gradient approximation (GGA) we have chosen for such estimates.

Our calculations indicate an even more complex behaviour of In_2O_3 at high pressures (see Figure 4). We find another polymorph that should become the most stable for pressures above 10.5 GPa. This high-pressure modification of In_2O_3 is iso-structural to the high-pressure modification of Rh_2O_3-II[42] with orthorhombic structure (space group *Pbna*, No 60). It's appearance in the In_2O_3 phase diagram is not surprising, because it happens to be a high-pressure phase of Al_2O_3 at about 96 GPa.[43] We also computed it as a possible high-pressure phase of Ga_2O_3 appearing at about 35 GPa. Astonishingly, this orthorhombic structure comes out lower in enthalpy than the corundum-type for pressures above 6.5 GPa—and that's even before the calculated cubic to hexagonal phase transition. It thus renders the corundum-type modification of In_2O_3 as being metastable throughout the entire enthalpy–pressure phase diagram.

How can we reconcile experimental results that show the existence of corundum-type In_2O_3 with our computational

results? First of all we observe from Figure 4 that for the pressure regime of interest, between 5 and 15 GPa, the computed enthalpy differences are smaller than 10 kJ mol^{-1}. Thus, entropy contributions arising from various sources can be expected to have significant impact on the free enthalpy difference ΔG between the compounds. Therefore, the additional term "$-T\cdot\Delta S$" will shift the relative stability of the phases and may eventually change the sequence of their appearance at higher pressure. For instance, differences in vibrational entropy can contribute some 5 kJ mol^{-1} to the free enthalpy of reaction at 1000 K. Moreover, we expect that defect chemistry contributes significantly as well. Some In atoms may not necessarily have oxidation state +3 but may also appear with oxidation state +1. Consequently, oxygen vacancies within the anion sub-structure are not unrealistic. The formation of the metastable corundum-type In_2O_3 under ambient pressure conditions can be related to the influence of organic solvents on the synthesis mechanism.[44, 45] It is known that the non-aqueous sol–gel routes may lead to the synthesis and stabilisation of the metastable phases as it was observed for the tetragonal ZrO_2.[46]

Conclusion

In summary, for the first time we have undoubtedly demonstrated, both theoretically and experimentally, the metastability of the corundum-type In_2O_3 polymorph. The In_2O_3 polymorph appears to be metastable throughout the entire enthalpy–pressure phase diagram. Upon heating the corundum-type In_2O_3 transforms irreversibly into cubic bixbyite-type In_2O_3 as shown by the STA as well as in situ heating XRPD experiments. This finding has particular significance for the synthesis of In_2O_3-based nanomaterials. It is also remarkably relevant to the understanding of the phase equilibria in the In_2O_3–SnO_2 (ITO) system. We are also confident that another high-pressure modification, orthorhombic Rh_2O_3-II-type, of In_2O_3 exists. Both the cubic bixbyite-type and the corundum-type modification of In_2O_3 should transform into this phase at pressures exceeding 15 GPa. This prediction calls for new high-pressure structural studies of In_2O_3.

Experimental Section

Synthesis: was performed by the modified non-alkoxide sol–gel method[23] based on the ammonia-induced hydrolysis of indium nitrate in methanol.

X-ray powder diffraction: The X-ray powder diffractogram was obtained in the Debye–Scherrer geometry by using a STOE STADI P diffractometer (Mo$_{K\alpha1}$ radiation) equipped with a position sensitive detector with 6° aperture. Intensity, $I(2\theta)$, versus diffraction angle 2θ from 5° to 45° was collected in steps of $\Delta(2\theta) = 0.02$°. The in situ heating XRD experiments (STOE IP-PSD with Imaging Plate detector, Mo$_{K\alpha1}$) were preformed on the powdered sample in a quartz glass capillary of 0.6 mm in diameter which was rotated in order to obtain a texture-free XRPD pattern. The heating was performed on line in a capillary furnace.

Simultaneous thermogravimetry/differential scanning calorimetry: Simultaneous thermogravimetry/differential scanning calorimetry (STA) with simultaneous gas analysis (mass spectrometry - QMS 403 C Aëolos, IPI and FTIR - Bruker Tensor27) was performed in oxygen (20 mL min^{-1})-argon (10 mL min^{-1}) mixture with heating rate 5 min^{-1} in Netzsch STA 449 C Jupiter®.

Computations: All calculations were carried out within the framework of density functional theory using the Vienna Ab Initio Simulation (VASP) package.[47–49] For optimisation and energy calculations we employed the generalised gradient approximation (GGA). Soft pseudopotentials describe the atomic cores; for Indium we explicitly included the d-electrons into the valence states. We relied further on Blöchls projector augmented wave (PAW) method. The cut-off energy (500 eV) for the expansion of the wave function into plane waves and the k-point meshes we used for sampling of the Brillouin zone ensured that the computed energy differences are converged to better than 1 meV per atom. We simulated pressure by reducing the volume of the unit cell, while optimizing atomic positions and lattice parameters simultaneously. The pressure p was calculated by a spline-fit to the energy-volume data, and the enthalpy was accessed through $dH = E + pV$. As is good practice, we plot the enthalpy relative to a reference structure, here we took that of the cubic In_2O_3 polymorph. Such computations have been very successful in the prediction of a new Rh_2O_3-type phase of alumina (Al_2O_3),[50,51] which has subsequently been experimentally realised.[43]

Note added in proof: While our manuscript was in press, we saw the computation (LDA) which predicted the transition from the corundum-to Rh_2O_3-II-type in In_2O_3 at 5 GPa.[52] Another work demonstrates the instability of corundum-type In_2O_3 above 300°C.[53]

Acknowledgements

[1] B. G. Hyde, S. Andersson, L. A. Bursill, M. O'Keeffe, *Nature Phys. Sci.* **1972**, *237*, 35.
[2] B. G. Hyde, S. Andersson, *Inorganic Crystal Structures*, Wiley, New York, **1989**.
[3] Y. A. Izyumov, V. N. Syromyatnikov, *Phase Transitions and Crystal Symmetry*, Kluwer, Dordrecht, **1990**.
[4] R. D. Shannon, *Solid State Commun.* **1966**, *4*, 629.
[5] A. F. Reid, A. E. Ringwood, *J. Geophys. Res.* **1969**, *74*, 3238.
[6] C. T. Prewitt, R. D. Shannon, D. B. Rogers, A. W. Sleight, *Inorg. Chem.* **1969**, *8*, 1985.
[7] T. Atou, K. Kusaba, K. Fukuoka, M. Kikuchi, Y. Syono, *J. Solid State Chem.* **1990**, *89*, 378.
[8] H. Mizoguchi, P. M. Woodward, *Chem. Mater.* **2004**, *16*, 5233.
[9] A. Gurlo, N. Barsan, M. Ivanovskaya, U. Weimar, W. Göpel, *Sens. Actuators B* **1998**, *47*, 92.
[10] J. G. Lu, P. C. Chang, Z. Y. Fan, *Mater. Sci. Eng. R* **2006**, *52*, 49.
[11] W. J. Heward, D. J. Swenson, *J. Mater. Sci.* **2007**, *42*, 7135.
[12] T. Yamanaka, T. Nagai, T. Okada, T. Fukuda, *Z. Kristallogr.* **2005**, *220*, 938.
[13] S. Z. Karazhanov, P. Ravindran, P. Vajeeston, A. Ulyashin, T. G. Finstad, H. Fjellvag, *Phys. Rev. B* **2007**, *76*, 075129.
[14] J. Q. Xu, Y. P. Chen, Q. Y. Pan, Q. Xiang, Z. X. Cheng, X. W. Dong, *Nanotechnology* **2007**, *18*.
[15] Z. B. Zhuang, Q. Peng, J. F. Liu, X. Wang, Y. D. Li, *Inorg. Chem.* **2007**, *46*, 5179.
[16] Y. Hao, G. Meng, C. Ye, L. Zhang, *Cryst. Growth Des.* **2005**, *5*, 1617.
[17] D. B. Yu, S. H. Yu, S. Y. Zhang, J. Zuo, D. B. Wang, Y. T. Qian, *Adv. Funct. Mater.* **2003**, *13*, 497.
[18] C. L. Chen, D. R. Chen, X. L. Jiao, C. Q. Wang, *Chem. Commun.* **2006**, 4632.
[19] C. H. Lee, M. Kim, T. Kim, A. Kim, J. Paek, J. W. Lee, S. Y. Choi, K. Kim, J. B. Park, K. Lee, *J. Am. Chem. Soc.* **2006**, *128*, 9326.
[20] D. B. Yu, D. B. Wang, Y. T. Qian, *J. Solid State Chem.* **2004**, *177*, 1230.
[21] M. Sorescu, L. Diamandescu, D. Tarabasanu-Mihaila, V. S. Teodorescu, *J. Mater. Sci.* **2004**, *39*, 675.
[22] A. Malik, R. Nunes, R. Martins, *Mater. Res. Soc. Symp. Proc.* **1998**, *481*, 599.
[23] M. Epifani, P. Siciliano, A. Gurlo, N. Barsan, U. Weimar, *J. Am. Chem. Soc.* **2004**, *126*, 4078.
[24] A. Gurlo, N. Barsan, U. Weimar, M. Ivanovskaya, A. Taurino, P. Siciliano, *Chem. Mater.* **2003**, *15*, 4377.
[25] M. I. Ivanovskaya, P. A. Bogdanov, A. C. Gurlo, L. S. Ivashkevich, *Inorg. Mater.* **1998**, *34*, 257.
[26] G. Frank, R. Olazcuaga, A. Rabenau, *Inorg. Chem.* **1977**, *16*, 1251.
[27] B.-C. Kim, J.-J. Kim, S.-H. Chang, *Mater. Res. Soc. Symp. Proc.* **2000**, *581*, 27.
[28] D. B. Yu, D. B. Wang, J. Lu, Y. T. Qian, *Inorg. Chem. Commun.* **2002**, *5*, 475.
[29] D. B. Yu, W. C. Yu, D. B. Wang, Y. T. Qian, *Thin Solid Films* **2002**, *419*, 166.
[30] K. H. Seo, J. H. Lee, J. J. Kim, M. I. Bertoni, B. J. Ingram, T. O. Mason, *J. Am. Ceram. Soc.* **2006**, *89*, 3431.
[31] B. C. Kim, J. Y. Kim, D. D. Lee, J. O. Lim, J. S. Huh, *Sens. Actuators B* **2003**, *89*, 180.
[32] M. Ristic, S. Popovic, M. Tonkovic, S. Music, *J. Mater. Sci.* **1991**, *26*, 4225.
[33] A. Gurlo, M. Ivanovskaya, N. Barsan, U. Weimar, *Inorg. Chem. Commun.* **2003**, *6*, 569.
[34] M. Sorescu, L. Diamandescu, D. Tarabasanu-Mihaila, *J. Phys. Chem. Solids* **2004**, *65*, 1719.
[35] C. Y. Wang, V. Cimalla, H. Romanus, T. Kups, G. Ecke, T. Stauden, M. Ali, V. Lebedev, J. Pezoldt, O. Ambacher, *Appl. Phys. Lett.* **2006**, *89*.
[36] K. R. Reyes-Gil, E. A. Reyes-Garcia, D. Raftery, *J. Phys. Chem. C* **2007**, *111*, 14579.
[37] A. N. Christensen, N. C. Broch, *Acta Chem. Scand.* **1967**, *21*, 1046.
[38] B. N. Litvin, L. I. Ivanova, *Sov Phys Crystallogr* **1970**, *14*, 988.
[39] E. H. P. Cordfunke, E. F. Westrum, *J. Phys. Chem. Solids* **1992**, *53*, 361.
[40] E. H. P. Cordfunke, R. J. M. Konings, W. Ouweltjes, *J. Chem. Thermodyn.* **1991**, *23*, 451.
[41] C. N. R. Rao, K. J. Rao, *Phase Transitions in Solids*, McGraw-Hill, New York, **1978**.
[42] R. D. Shannon, C. T. Prewitt, *J. Solid State Chem.* **1970**, *2*, 134.
[43] J. F. Lin, O. Degtyareva, C. T. Prewitt, P. Dera, N. Sata, E. Gregoryanz, H. K. Mao, R. J. Hemley, *Nat. Mater.* **2004**, *3*, 389.
[44] V. G. Kessler, G. I. Spijksma, G. A. Seisenbaeva, S. Hakansson, D. H. A. Blank, H. J. M. Bouwmeester, *J. Sol–Gel Sci. Technol.* **2006**, *40*, 163.
[45] M. Niederberger, *Acc. Chem. Res.* **2007**, *40*, 793–800.
[46] A. Ayral, T. Assih, M. Abenoza, J. Phalippou, A. Lecomte, A. Dauger, *J. Mater. Sci.* **1990**, *25*, 1268.
[47] G. Kresse, J. Hafner, *Phys. Rev. B* **1993**, *47*, 558.
[48] G. Kresse, J. Hafner, *Phys. Rev. B* **1994**, *49*, 14251.
[49] G. Kresse, J. Furthmüller, *Comp. Haematol. Int. Comp. Mater. Sci.* **1996**, *6*, 15.
[50] F. C. Marton, R. E. Cohen, *Am. Mineral.* **1994**, *79*, 789.
[51] K. T. Thomson, R. M. Wentzcovitch, M. S. T. Bukowinski, *Science* **1996**, *274*, 1880.
[52] R. Caracas, R. E. Cohen, *Phys. Rev. B* **2007**, *76*, 184101.
[53] D. Chu, Y.-P. Zeng, D. Jiang, J. Xu, *Nanotechnology* **2007**, *18*, 435605.